Organic aerosol formation from the oxidation of biogenic hydrocarbons

Robert J. Griffin,[1] David R. Cocker III,[2] Richard C. Flagan,[1] and John H. Seinfeld[3]

Abstract. A series of outdoor chamber experiments has been used to establish and characterize the significant atmospheric aerosol-forming potentials of the most prevalent biogenic hydrocarbons emitted by vegetation. These compounds were also studied to elucidate the effect of structure on aerosol yield for these types of compounds. Because oxidation products partition between the gas and aerosol phases, the aerosol yields of the parent biogenic hydrocarbons depend on the concentration of organic aerosol into which these products can be absorbed. For organic mass concentrations between 5 and 40 μg m^{-3}, mass-based yields in photooxidation experiments range from 17 to 67% for sesquiterpenes, from 2 to 23% for cyclic diolefins, from 2 to 15% for bicyclic olefins, and from 2 to 6% for the acyclic triolefin ocimene. In these photooxidation experiments, hydroxyl and nitrate radicals and ozone can contribute to consumption of the parent hydrocarbon. For bicyclic olefins (α-pinene, β-pinene, Δ^3-carene, and sabinene), experiments were also carried out at daytime temperatures in a dark system in the presence of ozone or nitrate radicals alone. For ozonolysis experiments, resulting aerosol yields are less dependent on organic mass concentration, when compared to full, sunlight-driven photooxidation. Nitrate radical experiments exhibit extremely high conversion to aerosol for β-pinene, sabinene, and Δ^3-carene. The relative importance of aerosol formation from each type of reaction for bicyclic olefin photooxidation is elucidated.

1. Introduction

A variety of organic compounds are emitted to the atmosphere from both natural and agricultural plants [*Isidorov et al.*, 1985; *Arey et al.*, 1991b; *Fehsenfeld et al.*, 1992; *Winer et al.*, 1992; *Arey et al.*, 1995]. Isoprene (C_5H_8), monoterpenes ($C_{10}H_{16}$), and sesquiterpenes ($C_{15}H_{24}$) comprise the majority of these emissions, although oxygenated and sulfur-containing species have also been identified [*Arey et al.*, 1991a; *König et al.*, 1995; *Puxbaum and König*, 1997]. Estimates of biogenic organic emissions have been made on global, national (e.g., the United States), and regional (e.g., the South Coast Air Basin of California or the Mediterranean region) bases. Total annual global biogenic organic emissions are estimated to range from 491 to 1150 TgC, greatly exceeding the 98 TgC of total organics estimated to be emitted from anthropogenic sources [*Müller*, 1992; *Guenther et al.*, 1995]. Averaged over the United States, biogenic emissions are estimated to be of the same order of magnitude of those from anthropogenic sources [*Lamb et al.*, 1993].

Significant uncertainty exists concerning the atmospheric reaction mechanisms of biogenic organics. The presence of unsaturated carbon-carbon bonds in these molecules leads to high reactivities [*Atkinson et al.*, 1995; *Shu and Atkinson*, 1995; *Atkinson*, 1997]. Because of the large quantity of emission and because of their atmospheric reactivity, biogenic nonmethane hydrocarbons (NMHCs) are predicted to play an important role in tropospheric chemistry [*Chameides et al.*, 1988; *McKeen et al.*, 1991; *Roselle et al.*, 1991; *Fehsenfeld et al.*, 1992]. Numerous studies investigating the nature of both gas-phase and aerosol-phase products formed from the reactions between biogenic NMHCs and the hydroxyl radical (OH), ozone (O_3), the O(^3P) atom, and the nitrate radical (NO_3) have been performed [*Stephanou and Stratigakis*, 1993; *Hakola et al.*, 1994; *Calogirou et al.*, 1995, 1997; *Berndt et al.*, 1996; *Grosjean and Grosjean*, 1997; *Hallquist et al.*, 1997; *Shu et al.*, 1997, *Vinckier et al.*, 1997; *Wängberg et al.*, 1997; *Alvarado et al.*, 1998; *Aschmann et al.*, 1998; *Griesbaum et al.*, 1998; *Yu et al.*, 1998].

Went [1960] was apparently the first to suggest the role of biogenic hydrocarbons in the formation of tropospheric aerosols. Higher molecular weight tropospheric hydrocarbons have been shown, upon oxidation, to produce semivolatile products that partition between the gas and aerosol phases [*Pandis et al.*, 1991; *Zhang et al.*, 1992; *Odum et al.*, 1996, 1997a, b; *Hoffmann et al.*, 1997]. In the aerosol phase, these products are referred to as secondary organic aerosol (SOA). Among anthropogenic NMHCs, aromatics are the most important source of SOA [*Odum et al.*, 1996, 1997a, b]. Among biogenic hydrocarbons, isoprene, because of its small size and the high volatility of its oxidation products, has been shown not to produce SOA at atmospheric levels [*Pandis et al.*, 1991]. Biogenic NMHCs larger than isoprene, however, are effective sources of aerosol [*Pandis et al.*, 1991; *Zhang et al.*, 1992; *Odum et al.*, 1996; *Hoffmann et al.*, 1997].

The importance of biogenic NMHCs in tropospheric aerosol formation will vary from area to area depending on climate, amount and nature of vegetation, and other

[1]Department of Chemical Engineering, California Institute of Technology, Pasadena.

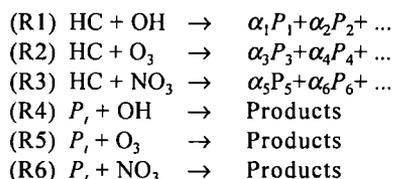[2]Department of Environmental Engineering Science, California Institute of Technology, Pasadena.

[3]Division of Engineering and Applied Science and Department of Chemical Engineering, California Institute of Technology, Pasadena.

environmental factors. In a Canadian forest, formation and growth of new particles have been attributed to oxidation of biogenic organics [*Leaitch et al.*, 1998]. It has been estimated that under peak photochemical conditions, anywhere from 20-80% of the organic aerosol burden in the South Coast Air Basin of California is secondary in nature [*Turpin and Huntzicker*, 1995; *Schauer et al.*, 1996] and that 16% of the SOA during a specific high-smog episode could be attributed to biogenic precursors [*Pandis et al.*, 1992]. Moreover, *Kaplan and Gordon* [1994] showed that a significant fraction of organic carbon associated with fine particulate matter in the Los Angeles area is not derived from fossil fuel precursors.

Previous experiments have provided limited information on the yields of SOA from α-pinene and β-pinene [*Pandis et al.*, 1991; *Zhang et al.*, 1992]. *Hoffmann et al.* [1997] reported the aerosol-forming potentials of a few other biogenic hydrocarbons, but too few experiments were performed to completely and quantitatively describe resulting aerosol formation. This study reports comprehensive outdoor chamber experiments on aerosol formation from 14 of the most prevalent biogenic organics. Differences in observed aerosol yields among compounds will be addressed on the basis of structural characteristics of the parent hydrocarbon. In sunlight-irradiated chamber experiments, OH, O_3, and NO_3 all contribute to hydrocarbon consumption and subsequent aerosol formation. To determine the individual contribution of each oxidant to aerosol formation for a parent hydrocarbon, gas-phase chemistry is modeled, from which the fraction of the parent hydrocarbon reacting with each oxidant can be determined. This is coupled with experiments in which O_3 or NO_3 is the only available oxidant. By deriving the quantitative parameters describing aerosol formation in these O_3-only or NO_3-only systems, it is possible to unravel the contribution to aerosol formation from each oxidant in full photooxidation experiments. An explanation of the mechanism of SOA formation, a derivation of the functional expression for aerosol yield, an expanded and specific list of the experiments performed, and a detailed experimental protocol all precede the presentation of data from these experiments and the corresponding analysis and discussion.

2. Mechanism of Secondary Organic Aerosol Formation

Consider a parent hydrocarbon, HC, reacting with OH, O_3, and NO_3. A variety of products form:

(R1) HC + OH   → $\alpha_1 P_1 + \alpha_2 P_2 + ...$
(R2) HC + O_3 → $\alpha_3 P_3 + \alpha_4 P_4 + ...$
(R3) HC + NO_3 → $\alpha_5 P_5 + \alpha_6 P_6 + ...$
(R4) P_i + OH   →   Products
(R5) P_i + O_3 →   Products
(R6) P_i + NO_3 →   Products

While only two products are indicated for each reaction here, the actual number of products is much greater. (Later, a two-product model is used to quantitatively describe aerosol formation in full photooxidation experiments or ones in which a single oxidant is available.) The parameter α_i represents a stoichiometric factor relating the total amount of product i formed to the total amount of hydrocarbon that reacts. Later, this constant will be expressed on a mass basis, rather than the

usual molar basis. As shown in (R4)-(R6), any of these products can, in principle, further react with any of the available oxidants, creating an even more complex and diverse mix of oxidation products.

For parent hydrocarbons containing roughly six or more carbon atoms, these products are semivolatile and, in the presence of sufficient organic aerosol, will partition between the gas and aerosol phases. The fraction of each product that partitions to the aerosol phase can be described on the basis of an equilibrium coefficient $K_{om,i}$. In principle, if the molecular nature of each product, as well as that of the aerosol organic phase, were known, $K_{om,i}$ could be calculated from first principles. In practice, such molecular-level information is not available, so $K_{om,i}$ values are determined experimentally.
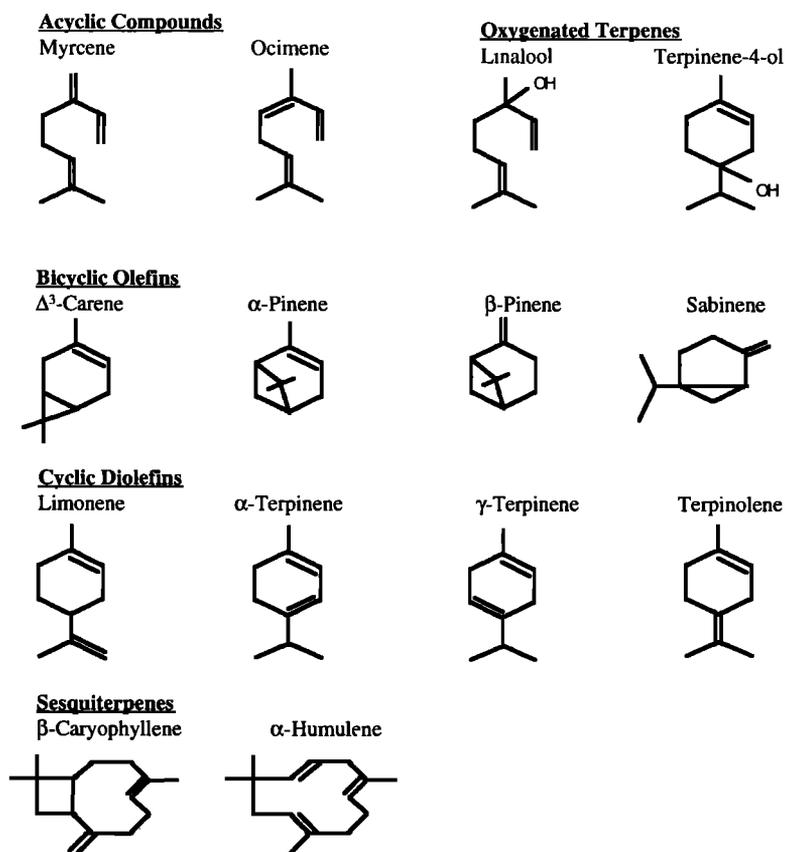
3. Fractional Aerosol Yield

Secondary organic aerosol formation has been determined experimentally through investigation of the fractional aerosol yield Y [*Pandis et al.*, 1991; *Zhang et al.*, 1992; *Odum et al.*, 1996, 1997a, b; *Hoffmann et al.*, 1997]. Because identification and quantification of individual oxidation products, for example, all the individual products in (R1)-(R6), are difficult, this yield is a convenient overall measure of the aerosol-forming potential of the secondary products of atmospheric oxidation of a parent organic molecule. This yield is defined as the ratio of the amount of SOA formed from the oxidation of a given parent compound to the amount of that compound that reacted:

$$Y = \frac{\Delta M_o}{\Delta HC} \tag{1}$$

where ΔM_o ($\mu g \ m^{-3}$) is the organic aerosol mass formed after the consumption of ΔHC ($\mu g \ m^{-3}$) of the given parent. The extent of gas/particle absorptive partitioning depends on the amount of the condensed organic phase into which the products can be absorbed. Thus aerosol yield depends on the amount of organic matter present, M_o, into which the semivolatile products may partition. An outcome of this mechanism is that a secondary product can be absorbed into an organic phase, even if it exists in the gas phase below its own saturation concentration [*Pankow*, 1994a, b; *Odum et al.*, 1996, 1997a, b; *Hoffmann et al.*, 1997]. *Pankow* [1994a, b] has defined an absorption equilibrium coefficient $K_{p,i}$ ($m^3 \ \mu g^{-1}$) for the partitioning of such a semivolatile component between the gas and particle phases as

$$K_{p,i} = \frac{F_{i,om}/(TSP)}{A_i} = \frac{760RTf_{om}}{M_{om}10^6 \zeta_i p_{L,i}^o} \tag{2}$$

where $F_{i,om}$ (ng m^{-3}) is the mass concentration of compound i in the absorbing organic matter (*om*) phase, A_i (ng m^{-3}) is its gas-phase mass concentration, TSP ($\mu g \ m^{-3}$) is the total suspended particulate concentration, R is the ideal gas constant, T (K) is the temperature, f_{om} is the fraction of the TSP that is absorbing *om*, M_{om} (g mol^{-1}) is the mean molecular weight of the absorbing phase, ζ_i is the activity coefficient of species i in the *om* phase, and $p_{L,i}^o$ (torr) is the vapor pressure (subcooled, if necessary) of compound i at temperature T. If only the absorbing organic phase is considered, a similar equilibrium constant can be defined as

Acyclic Compounds
Myrcene   Ocimene

Oxygenated Terpenes
Linalool   Terpinene-4-ol

Bicyclic Olefins
Δ^3-Carene   α-Pinene   β-Pinene   Sabinene

Cyclic Diolefins
Limonene   α-Terpinene   γ-Terpinene   Terpinolene

Sesquiterpenes
β-Caryophyllene   α-Humulene

Figure 1. Chemical structures of the biogenic hydrocarbons investigated. Bonds between carbon atoms are shown with vertices representing carbon atoms; hydrogen atoms bonded to carbon are not explicitly shown.

$$K_{om,i} = \frac{F_{i,om}}{A_i M_o} = \frac{K_{p,i}}{f_{om}} \tag{3}$$

simply by dividing $K_{p,i}$ by f_{om}. Equation (3) indicates that this new equilibrium constant is a function of the mass of the available organic phase into which a semivolatile product can be absorbed. Thus more of each product partitions to the organic aerosol phase as the total organic aerosol concentration increases. As a result, a parent compound that has undergone a certain amount of photooxidation, ΔHC, will exhibit a range of SOA yield values depending on the value of M_o. For the experiments described in this paper, $M_o = \Delta M_o$, since all organic aerosol mass is generated by the oxidation of the parent hydrocarbon. By combing the definitions of Y and $K_{om,i}$, a total mass balance, and a stoichiometric constraint, Y can be expressed as a function of ΔM_o by [Odum et al., 1996]

$$Y = \Delta M_o \sum_i \left(\frac{\alpha_i K_{om,i}}{1 + K_{om,i} \Delta M_o}\right) \tag{4}$$

where ΔM_o, $K_{om,i}$, and α_i are defined as above. Yield data for over 30 individual parent compounds obtained in the Caltech outdoor chamber have been fit to (4) using a two product model, that is, with parameters, α_1, α_2, $K_{om,1}$ and $K_{om,2}$ [Hoffmann et al., 1997; Odum et al., 1996, 1997a, b]. While it was given earlier that many products result from the atmospheric oxidation of a parent hydrocarbon, it has been shown that a two-product model is needed for most

compounds to accurately describe the shape of the yield curve described by (4). Use of three or more products in the model has been proven to be superfluous. The four parameters derived in the two-product model can be seen as an adequate description of the stoichiometry and volatility of the complex mix of oxidation products.

It must be noted that this theory assumes that secondary products are unable to form a solution with existing seed aerosol. Accounting for the interactions between the organic compounds themselves allows it to be shown that such products can condense onto seed aerosol at concentrations lower than those predicted by saturation theory alone [Seinfeld and Pandis, 1998]. In this case, the threshold amount of the parent compound that must react to form SOA in the chamber is defined as ΔHC^*. After consumption of ΔHC^*, products condense onto seed aerosol to form an initial amount of SOA, which can then act as an absorptive medium. At this point, absorption becomes the dominant mechanism governing the partitioning of secondary products and, therefore, determining SOA yield, as in the atmosphere.

4. Chamber Studies

In this study the results of extensive outdoor chamber experiments on aerosol formation from 14 biogenic organic compounds are reported. These compounds include monoterpenes of chemical formula $C_{10}H_{16}$: α-pinene, β-pinene, Δ^3-carene, and sabinene, bicyclic olefins that differ in the

Table 1. Reaction Rate Constants for the Oxidation of Biogenic Hydrocarbons

Parent	$k_{OH} \times 10^{12}$	$k_{O_3} \times 10^{18}$	$k_{NO_3} \times 10^{12}$
Δ^3-Carene	88	37	9.1
β-Caryophyllene	197	11600	19
α-Humulene	293	11700	35
Limonene	171	200	12 2
Linalool	159	430	11 2
Myrcene	215	470	11
Ocimene	252	540	22
α-Pinene	53.7	86.6	6.2
β-Pinene	78.9	15	2 5
Sabinene	117	86	10
α-Terpinene	363	21100	140
γ-Terpinene	177	140	29
Terpinene-4-ol	170	250	14.6
Terpinolene	225	1880	97

Units are cm^3 molecule^{-1} s^{-1}. Data are from *Atkinson et al.* [1995], *Shu and Atkinson* [1995], and *Atkinson* [1997].

location of the double bond and the number of carbons associated with the secondary ring; limonene, α-terpinene, γ-terpinene, and terpinolene, cyclic diolefins that differ only in the location of a second double bond; and myrcene and ocimene, acyclic triolefins that differ only in the location of a third double bond. In addition, two sesquiterpenes of structure $C_{15}H_{24}$ (β-caryophyllene and α-humulene) and two oxygenated terpenes (linalool and terpinene-4-ol) are investigated. The structure of each of these compounds is shown in Figure 1, and their reaction rate constants at 298K with OH, O_3, and NO_3 are given in Table 1.

As noted above, full sunlight-irradiated photooxidation experiments will have, in general, all three of OH, O_3, and NO_3 present, and, therefore, in general, aerosol yields will be the result of products generated in all three oxidation pathways. Experiments performed in a dark system with O_3 or NO_3 as the only available oxidants, in conjunction with results from gas-phase modeling, can then be used to determine the individual contributions to SOA formation from each oxidant. Experiments involving NO_3 as the only oxidant need be performed only for bicyclic olefins, as they are the slowest reacting of the compounds studied and will persist long enough for NO_3 to build up in the chamber. The other compounds are consumed completely by OH and O_3 in the sunlight-driven photooxidations prior to significant formation of NO_3.

5. Experimental Procedure

All experiments were performed in a sealed, 50-m^3 Teflon chamber that has been described in detail previously [*Odum et al*, 1996, 1997a, b; *Hoffmann et al*, 1997]. This chamber was normally divided in the center so that two experiments could be run under identical environmental conditions. Each resulting chamber had an estimated volume of 20 m^3. Instruments for monitoring gas-phase components and a computer for acquiring aerosol data were operated from a laboratory adjacent to the chamber. Aerosol sampling

instruments were operated directly next to the chamber in a closed cart that was maintained at a temperature of approximately 25°C. Between experiments, the chamber was continuously purged with compressed air and allowed to bake in sunlight for at least a day. The compressed air was purified to remove organics, particulate matter, water, and NO_x species. Air in the chamber prior to the experiments contained no detectable hydrocarbons or particles and less than 5 ppb NO_x. Before entering the chamber, the air was passed through a rehumidifier containing distilled and deionized water so that the relative humidity during the experiments was approximately 5%.

At this time, it has not been determined how an increase in humidity influences the formation of SOA. Possible effects include differences in the chemical and physical nature of the absorbing phase such as a shift from an organic mixture to an aqueous-inorganic-organic mixture, a variation in the mean molecular weight of the absorbing phase, and a change in the activities of secondary products in the absorbing mixture. Deviation in any or all of these factors would affect the equilibrium partitioning coefficient of each product, thereby affecting the overall SOA yield. These issues are currently under study.

Gas-phase concentrations of the parent hydrocarbons in the chamber were monitored using a Hewlett Packard (Palo Alto, California) 5890 gas chromatograph (GC) equipped with a DB-5 column (J&W Scientific, Davis, California) and a flame ionization detector (FID). The temperature program for the GC began at -60°C, held for 1 min, ramped from -60°C to 150°C at a rate of 40°C min^{-1}, and then held for 1.5 min. Prior to each experiment, known volumes of a solution of the parent hydrocarbon and methylene chloride were vaporized into a small, 60-L Teflon bag filled with compressed air. Measurements from these bags were then used to calibrate the GC.

Following the GC calibration, seed particles of $(NH_4)_2SO_4$ were injected into the chamber to obtain initial particle concentrations of approximately 5,000-10,000 particles cm^{-3}. (Seed particles were not used in nitrate radical experiments.) The particles were generated by atomizing a solution of $(NH_4)_2SO_4$ salt in deionized water. The particles flowed through a heated copper tube and a diffusion dryer, resulting in crystalline $(NH_4)_2SO_4$, and were then passed through a ^{85}Kr neutralizer before being injected into the chamber. The initial size distribution of the seed aerosol was centered around a diameter of approximately 100 nm.

Once the number concentration of particles on each side of the chamber had equilibrated, the chamber was divided and covered with a black polyethylene tarpaulin in order to prevent sunlight from irradiating the contents of the chamber. Propene, NO, NO$_2$, hexafluorobenzene (C_6F_6), and hydrocarbon were then injected into each side of the chamber through Teflon lines. Propene was used as a photochemical initiator to provide sufficient levels of OH, and C_6F_6 was used as a nonreactive internal standard. NO and NO$_2$ are added primarily to facilitate the basic photochemical cycle involving O_3 and to participate in the reaction converting peroxy radicals (RO_2) to alkoxy radicals (RO). Therefore it is expected that the NO_x level in the chamber will have little effect on aerosol yield except through the formation of O_3 and NO_3. Propene and NO_x were injected from certified cylinders of approximately 500 ppm in nitrogen. The target initial mixing ratio of propene in each chamber was 250-300 ppb for each

Table 2a. Initial Conditions and Data for Photooxidation Experiments

Date	Parent	T, K	ΔHC, ppb	ΔM_o, μg m^{-3}	Y	NO, ppb	NO$_2$, ppb
07/01/97a	Δ^3-Carene	310.0	28.8	2 5	0 016	36.9	55.4
07/01/97b	Δ^3-Carene	310 0	66 8	11.6	0 033	90 5	96 9
08/21/97b	Δ^3-Carene	312 8	72 5	54 6	0.142	67 5	60.8
08/15/97b	Δ^3-Carene	308 8	73 6	63 7	0 161	86 2	82 3
08/19/97b	Δ^3-Carene	312.0	104 6	99 7	0.179	89 6	72 3
09/18/97b	β-Caryophyllene	308 3	5 9	17 6	0.369	18 7	9.4
09/16/97b	β-Caryophyllene	306 6	10 3	64.6	0 775	39 0	14.9
09/17/98b	β-Caryophyllene	308.6	12 9	82 3	0 790	13 1	11 1
09/18/97a	α-Humulene	308 3	5 0	12 9	0 319	16.2	7.8
09/15/97b	α-Humulene	309 3	5 4	28 2	0.648	30 8	23.8
09/16/97a	α-Humulene	306 6	8 6	59.2	0.845	37 6	14 8
09/17/97a	α-Humulene	308 6	9 2	54 2	0 732	19 5	13 5
08/26/97b	Limonene	313 4	20 6	9.5	0 087	43.1	61 8
08/26/97a	Limonene	313 4	35 2	49 6	0.266	17.4	62.8
08/17/97b	Limonene	309.4	49.5	79.1	0.298	73.6	65 8
08/17/97a	Limonene	309.4	65.1	120 2	0 344	75.7	64.4
08/28/97b	Linalool	312.4	71 6	26 7	0.056	164 7	130.1
09/19/97a	Myrcene	311 1	9 8	3 5	0 068	23.5	21.5
09/10/97b	Myrcene	311.9	77.5	57.5	0 168	117.9	79 9
08/24/97a	Ocimene	313 2	45 6	7 3	0.030	96.3	85.7
07/23/97a	Ocimene	315.7	76.5	17 6	0.043	49.0	94 0
07/23/97b	Ocimene	315 7	142.0	50 3	0 066	125.1	168 6
08/15/97a	β-Pinene	308.8	32.3	20 4	0.118	81.4	53 4
07/15/97a	β-Pinene	313 6	33 7	14.6	0 080	49.2	62.5
07/17/97a	β-Pinene	316.2	42 0	7.2	0.032	15 6	43.4
07/27/97a	β-Pinene	313 3	45 0	34.2	0.144	53 1	58.6
07/15/97b	β-Pinene	313 6	62 2	51 4	0.153	87 0	79.7
08/19/97a	β-Pinene	312.0	79 0	109.4	0 260	88 8	64 8
07/21/97a	β-Pinene	313 5	85.5	100.1	0 221	93.7	63 6
07/21/97b	β-Pinene	313 5	96 5	141 6	0.272	93 0	67 0
07/09/97a	Sabinene	316.0	13 9	1.9	0.025	21 3	43.5
07/07/97a	Sabinene	310 3	34 9	14.3	0.076	50.2	52.2
07/05/97a	Sabinene	312 9	53.3	23.9	0.085	91.9	81 4
08/24/97b	Sabinene	313.2	74 0	48.7	0.124	115 3	96.5
07/05/97b	Sabinene	312 9	75 3	51.4	0.129	93 2	61.4
07/07/97b	Sabinene	310 3	77 7	53.4	0.129	106.0	77.9
07/09/97b	Sabinene	316.0	83.3	65 2	0 145	115.5	84.1
09/04/97a	α-Terpinene	316.0	47 0	20 2	0 082	87.1	51 3
09/08/97a	α-Terpinene	314 7	65 2	43.9	0.128	62.8	148.9
09/06/97a	α-Terpinene	313.3	79 6	73.8	0.175	106 0	53.0
09/11/97a	γ-Terpinene	312.4	40.9	21 3	0.098	44 7	45 0
09/10/97a	γ-Terpinene	311 9	77.5	65.9	0 160	132.2	82.7
09/06/97b	Terpinene-4-ol	313 3	116.2	42.6	0.056	216.3	132.2
09/02/97a	Terpinolene	312 6	25 0	1.9	0.015	47 7	47.3
09/02/97b	Terpinolene	312 6	46.9	5 2	0 021	42.4	64.7
08/28/97a	Terpinolene	312 4	60 1	9.9	0.031	54.7	56.3
09/11/97b	Terpinolene	312 4	92 3	17 8	0.036	128 0	88.8
09/04/97b	Terpinolene	316 0	133 2	28.9	0.041	190.5	122.7

Read 09/18/97 as September 18, 1997.

photooxidation experiment, and the amount of NO$_x$ (NO$_x$ = NO + NO$_2$) injected varied depending on the initial concentration of the parent hydrocarbon. The average hydrocarbon to total NO$_x$ ratio (ppbC/ppb) was approximately 5 to 1, whereas the average ratio of NO to NO$_2$ was 1.5 to 1. The parent hydrocarbon and the C$_6$F$_6$ were injected by vaporizing

microliter quantities in a heated glass bulb that was diluted with compressed, purified air that flowed directly to the chamber.

After all of the injections to the chamber had been made and sufficient time had passed to allow mixing within each side of the chamber, measurements of hydrocarbon, O$_3$, NO$_x$,

Table 2b. Initial Conditions and Data

Date	Parent	T, K	ΔHC, ppb	ΔM_o, μg m^{-3}	Y
Nitrate Radical Experiments					
05/20/98a	Δ^3-Carene	308 0	36.2	24 4	0 125
06/03/98a	Δ^3-Carene	308.2	51 6	178.8	0.643
05/28/98a	Δ^3-Carene	310 1	70.2	267 7	0 713
05/18/98a	Δ^3-Carene	309.2	80 1	310.5	0.722
06/01/98a	β-Pinene	309 9	18.8	32.4	0 322
05/09/98b	β-Pinene	304.0	19 7	46.1	0.428
06/01/98b	β-Pinene	309.9	54 7	243 2	0.830
05/13/98b	β-Pinene	302.0	96.4	467.3	0 891
05/20/98b	Sabinene	308.0	32.8	24 3	0.138
06/03/98b	Sabinene	308 2	41 5	151.5	0.677
05/28/98b	Sabinene	310 1	55.9	223.9	0 749
05/18/98b	Sabinene	309.2	68 2	276 5	0.755
Ozone Experiments					
06/19/98b	Δ^3-Carene	308 6	11.8	5.5	0.086
06/21/98b	Δ^3-Carene	309 3	29.9	18.7	0 117
06/23/98b	Δ^3-Carene	307.0	47.7	33.1	0 129
06/15/98b	Δ^3-Carene	306.2	89.9	64.4	0 132
06/05/98a	α-Pinene	309.9	16.7	7.4	0.083
06/05/98b	α-Pinene	309.9	18 2	8 5	0.087
06/07/98a	α-Pinene	303 3	31.0	30 3	0 179
06/07/98b	α-Pinene	303.3	45.5	46 0	0.184
06/09/98a	α-Pinene	308.0	57 0	52 3	0.170
06/09/98b	α-Pinene	308.0	65 0	65 1	0.186
06/13/98a	β-Pinene	308 4	11 9	0 0	0 000
06/13/98b	β-Pinene	308.4	35.2	1 8	0 009
06/11/98a	β-Pinene	306 9	57.6	9.2	0 030
06/11/98b	β-Pinene	306 9	80.1	22 5	0.052
06/19/98a	Sabinene	308 6	12.5	1.4	0.021
06/21/98a	Sabinene	309.3	34 0	5 1	0.028
06/23/98a	Sabinene	307.0	51 6	9 1	0.033
06/15/98a	Sabinene	306 2	92.4	17.9	0 036

and particle concentrations were taken in order to obtain initial values and to ensure that the contents of the chamber were well mixed. Typically, three hydrocarbon reading using the GC method described above were taken from each side of the chamber. Ozone was measured using a Dasibi Environmental Corporation (Glendale, California) Model 1008-PC O_3 analyzer that was calibrated at the beginning of the series of experiments by Dasibi. The estimated uncertainty in these readings is ±4%; a drift of only a few percent in the monitor readings was seen over the course of several months. NO, NO_2, and total NO_x concentrations were monitored using a Thermo Environmental Instruments (Franklin, Massachusetts) Model 42 chemiluminescence NO_x monitor. Prior to each experiment, zero and span checks were performed on this instrument using certified cylinders of NO, NO_2, and N_2. The estimated uncertainty in NO_x monitor readings are ±4% for NO and ±7% for NO_2. After the initial readings were complete, the black tarpaulin was removed, exposing the chamber to sunlight and starting the experiment. During the experiments, O_3 and NO_x were sampled continuously from each

side of the chamber in intervals of 10 min, and hydrocarbon samples were taken throughout the experiment from alternating sides of the chamber. Temperature was also tracked continuously throughout the course of each experiment.

Aerosol data included size distributions and total number concentrations for each side of the chamber at a 1-min frequency. Aerosol instrumentation consisted of a TSI (St. Paul, Minnesota) Model 3071 cylindrical scanning electrical mobility spectrometer (SEMS) to measure the size distribution of particles and a TSI Model 3760 condensation nucleus counter (CNC) to count particles. SEMS voltages were ramped exponentially from 40 to 8500 V, and the classifier flows were 2.5 L min^{-1} for sheath and excess flows and 0.25 L min^{-1} for inlet and classified aerosol flows. This allowed for the measurement of particles in the diameter range of approximately 30-850 nm. A complete and detailed description of the SEMS operation that includes a description of data analysis techniques has been published previously [*Wang and Flagan*, 1990].

Experiments in which O_3 or NO_3 is the primary oxidant

were performed at night to eliminate the possibility of photolysis of secondary products to form OH (This also avoided high temperatures caused by keeping the chamber covered with the black tarpaulin in direct sunlight, as in the experiments of *Hoffmann et al.*, [1997].) In ozonolysis experiments, an appropriate concentration of 2-butanol was used to scavenge any OH formed in the hydrocarbon-O_3 reaction and to ensure that O_3 was the only oxidant present in the system [*Chew and Atkinson*, 1996].

To compare aerosol formation under the different conditions, it is important that the temperature in the chamber during the dark experiments be close to that of a typical afternoon smog chamber experiment because the partitioning coefficient $K_{om,i}$ is a function of temperature. To achieve this, the entire chamber was covered with an insulating cover as well as the black tarpaulin, neither of which was removed during the course of the experiment. This was done after the seed particles had been injected and the chamber had been divided as described above. In addition, four Holmes (Milford, Massachusetts) Model HFH-501FP space heaters were placed in the open area underneath the chamber. By varying the number of heaters used and their power settings, daytime temperatures of approximately 30°-35°C could be achieved and maintained throughout the course of an experiment.

Injections of hydrocarbon, C_6F_6, and 2-butanol (if needed) were then made to each side as described above. Once initial readings for both sides had been completed for ozonolysis experiments, O_3 was injected to each side using an Enmet Corporation (Ann Arbor, Michigan) Model 04052-011 O_3 generator until the Dasibi O_3 monitor read approximately 4 times the initial hydrocarbon concentration on the appropriate side. For NO_3 experiments, sufficient NO_3 was generated via the thermal decomposition of N_2O_5 synthesized by the combination of O_3 and NO_2 (*R. Atkinson*, personal
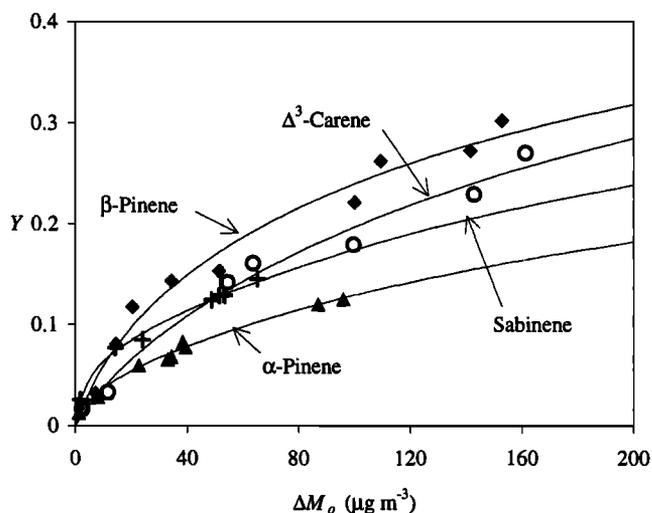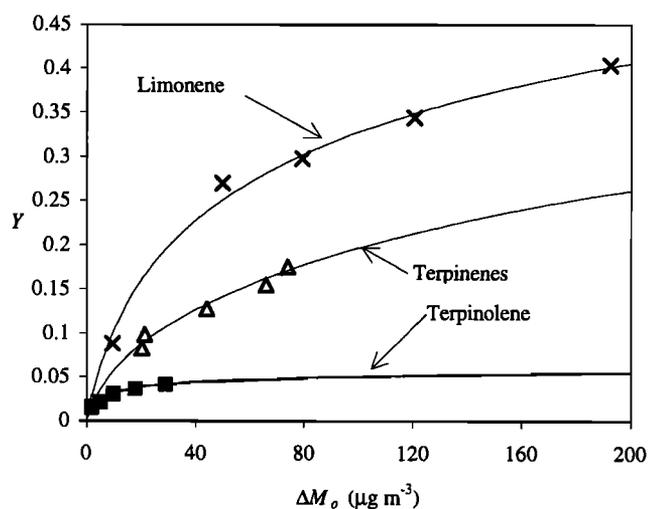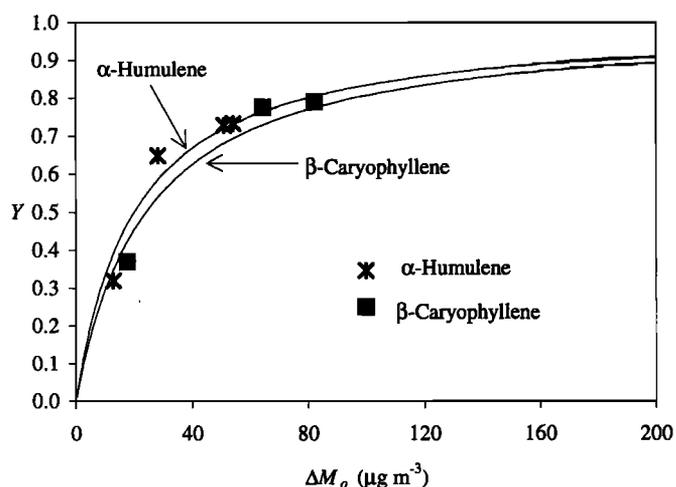

Figure 3. Secondary organic aerosol yields (data and fitted curves) for the cyclic diolefins tested as a function of organic mass concentration in photooxidation experiments. The α_1, α_2, $K_{om,1}$, and $K_{om,2}$ values used to generate the two-product model lines are given in Table 3. Some data were taken from *Hoffmann et al.* [1997].

communication, 1997). Continuous aerosol, GC, and temperature readings were taken as described above. Initial conditions and resulting data are given for all experiments in Table 2.
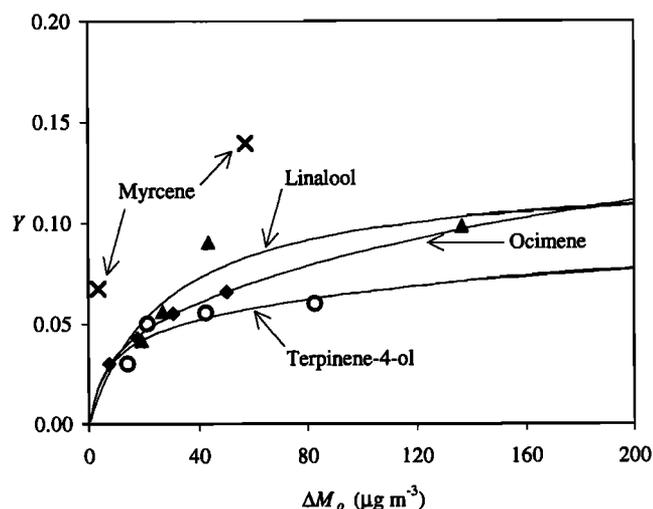
6. Yields of Biogenic Organics in Photo-oxidation Experiments

Figures 2-5 show aerosol yields as a function of organic mass concentration for photooxidation experiments with the 14 biogenic compounds tested. Figures 2-5 also show the theoretical yield curves fit using (4) for each biogenic hydrocarbon. The parameters resulting from the fit of these curves are given in Table 3. As seen in Figures 2-5, there exists a wide range of aerosol yields for biogenic hydrocarbons. Sesquiterpenes have the highest yields of the compounds tested. This behavior is a consequence of the high carbon number of the parent compounds. Limonene, β-pinene, and sabinene are among the compounds with the highest yields, clearly indicating the effect of the presence of a =CH_2 group in a cyclic monoterpene structure. The yields of limonene, Δ^3-carene, α-pinene, and the terpinene isomers also indicate the significance of double bonds that are internal to ring structures. When oxidants attack unsaturated bonds, carbon atoms may be lost as a result of the decomposition of the resulting radical species [*Atkinson*, 1997]. However, the two trends noted above suggest that fewer carbon atoms are lost by oxidant attack on =CH_2 double bonds or double bonds that are internal to ring structures. The lower yields of ocimene, myrcene, linalool, and terpinolene also support this hypothesis since three or more carbon atoms can be cleaved by oxidant attack on these molecules. However, terpinene-4-ol, which has an OH group replacing the second double bond of the terpinene isomers, does not adhere to this trend, in that its yield is significantly lower than that of the terpinene isomers. This is likely a result of the fact that the OH group replaces the more reactive double bond.

Figure 2. Secondary organic aerosol yields for the bicyclic olefins tested as a function of organic mass concentration in photooxidation experiments. Data are shown as filled triangles, plus signs, open circles, and filled diamonds for α-pinene, sabinene, Δ^3-carene, and β-pinene, respectively. The α_1, α_2, $K_{om,1}$, and $K_{om,2}$ values used to generate the two-product model fitted curves are given in Table 3. Some data were taken from *Hoffmann et al.* [1997].

Figure 4. Secondary organic aerosol yields (data and fitted curves) for the sesquiterpenes tested as a function of organic mass concentration in photooxidation experiments. The α_1, α_2, $K_{om,1}$, and $K_{om,2}$ values used to generate the two-product model lines are given in Table 3. Some data were taken from *Hoffmann et al.* [1997].

Figure 5. Secondary organic aerosol yields (data and fitted curves) for the acyclic triolefins and oxygenated terpenes tested as a function of organic mass concentration in photooxidation experiments. The α_1, α_2, $K_{om,1}$, and $K_{om,2}$ values used to generate the two-product model lines are given in Table 3. Some data were taken from *Hoffmann et al.* [1997]. No curve is shown for myrcene as only two experiments with myrcene were performed.

For the bicyclic olefins, the number of carbon atoms associated with the secondary ring also seems to have an effect on SOA yield. Δ^3-carene and α-pinene have an identical structure, outside of a difference in the number of carbon atoms in the secondary ring, yet Δ^3-carene has a higher aerosol yield than α-pinene (Figure 2). Since many of the products of the oxidation of these parent hydrocarbons are expected to be similar and retain their secondary ring structures [*Yu et al.*, 1998], this difference in yield can be explained by the less volatile nature of Δ^3-carene (boiling point 168°-169°C) compared to α-pinene (boiling point 155°-156°C). However, sabinene (boiling point 163°-164°C), which has an exocyclic methylene group and a secondary three-carbon ring, has lower yields than β-pinene (boiling point 165°-167°C), which has an external methylene group and a secondary four-carbon ring. This is the opposite of the trend seen with Δ^3-carene and α-pinene. This difference cannot be explained by the slight difference in boiling point of the parent compounds. However, it can possibly be explained by a mechanism that results in the

cleavage of both rings in sabinene since open-chain compounds tend to be more volatile than cyclic ones. This mechanism, adapted from the H atom abstraction mechanism of *Aschmann et al.* [1998] for α-pinene, is shown in Figure 6. For illustrative purposes, only OH radical reaction is shown. The corresponding mechanism for β-pinene is much less likely to result in the cleavage of both rings.

7. Yields of Biogenic Organics in Ozonolysis and Nitrate Radical Experiments

In general, aerosol yields in ozonolysis of the biogenic hydrocarbons are less dependent on organic mass concentration when compared to those under sunlight-irradiated photooxidation, in which the parent hydrocarbon is oxidized by OH, O_3, and NO_3. This indicates that ozonolysis

Table 3. Aerosol Yield Parameters for the Photooxidation of Biogenic Hydrocarbons

| Parent	α_1	α_2	$K_{om,1}$, m³ µg⁻¹	$K_{om,2}$, m³ µg⁻¹
Δ^3-Carene*	0.054	0.517	0.043	0.0042
β-Caryophyllene*	1.000	-	0.0416	-
α-Humulene	1 000	-	0 0501	-
Limonene	0.239	0.363	0.055	0.0053
Linalool*	0.073	0 053	0.049	0 0210
Ocimene*	0.045	0.149	0.174	0.0041
α-Pinene*	0.038	0.326	0.171	0.0040
β-Pinene*	0.130	0.406	0.044	0.0049
Sabinene	0.067	0.399	0.258	0.0038
α- & γ-Terpinene	0.091	0.367	0.081	0.0046
Terpinene-4-ol*	0.049	0.063	0.159	0.0045
Terpinolene	0.046	0.034	0.185	0.0024

*Includes data from *Hoffmann et al.* [1997].
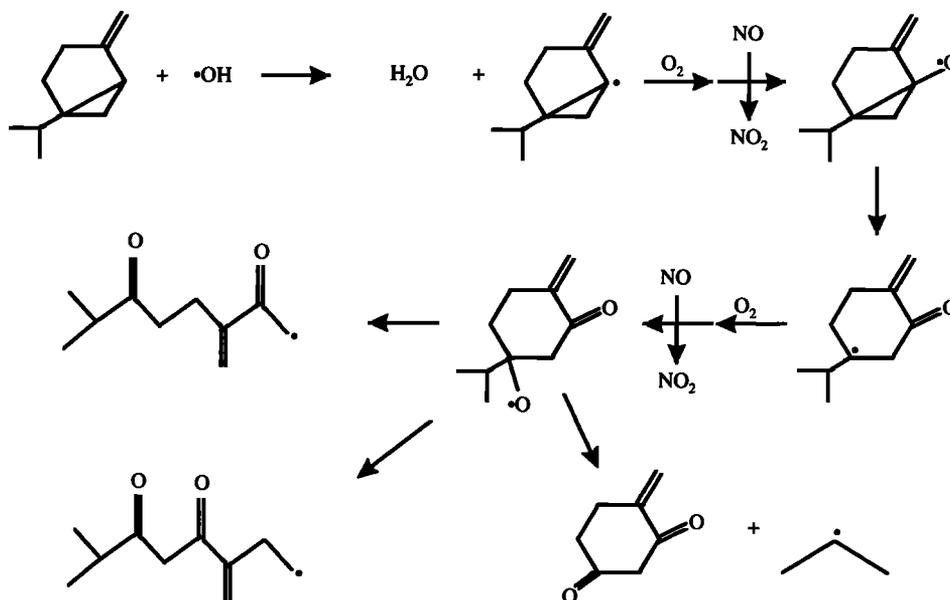
Figure 6. Possible ring-opening mechanism for the reaction between OH and sabinene.

leads to secondary products that are less volatile than those in the full photooxidation system [*Hoffmann et al.*, 1997]. O_3 reactions with β-pinene and sabinene, however, produce significantly lower aerosol yields than the corresponding full photooxidation experiments. The opposite behavior is seen for α-pinene and Δ^3-carene (Figure 7 and Table 4). This indicates that compounds with double bonds internal to ring structures are more likely to form condensable products when compared to compounds with external double bonds. (These results cannot be compared to those of *Hoffman et al.* [1997], since those experiments were performed without an OH scavenger and at considerably different temperatures.) Large yields of aerosol result from NO_3 reaction with β-pinene, Δ^3-carene, and sabinene, indicating possible formation of nitrated

products in large yields (Figure 8 and Table 4). The olefin α-pinene shows insignificant aerosol formation from NO_3 oxidation. This can be explained by the creation in high yield of pinonaldehyde, which is too volatile to partition significantly to the aerosol phase [*Wängberg et al.*, 1997].

Some scatter can be seen in the data sets associated with each type of experiment. This is most likely linked to the uncertainty regarding charging of the aerosol generated in the chamber and slight variations in temperature between experiments.

8. Contribution of Individual Oxidants to Aerosol Formation

To identify the amount of parent hydrocarbon consumed by each of the three available oxidants in sunlight-driven photooxidation experiments, the SAPRC90b mechanism [*Carter*, 1990] was used to model the gas-phase chemistry of the photochemical smog chamber experiments for α-pinene [*Odum et al.*, 1996; *Hoffmann et al.*, 1997], β-pinene,
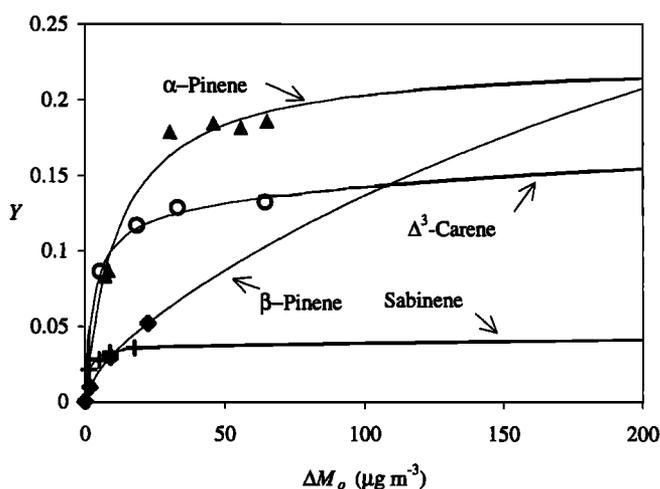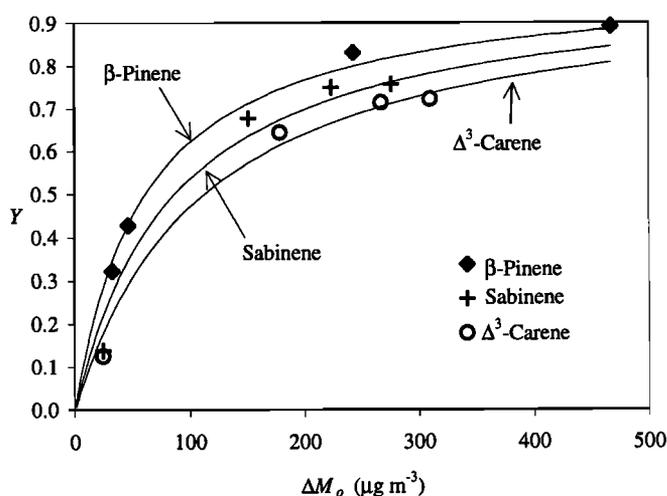

Figure 7. Secondary organic aerosol yields for the bicyclic olefins tested as a function of organic mass concentration in ozonolysis experiments. Data are shown as filled triangles, plus signs, open circles, and filled diamonds for α-pinene, sabinene, Δ^3-carene, and β-pinene, respectively. The α_1, α_2, $K_{om,1}$, and $K_{om,2}$ values used to generate the two-product model fitted curves are given in Table 4.

Table 4. Aerosol Yield Parameters for the Ozone and Nitrate Radical Oxidation of Bicyclic Olefins

Parent	α_1	α_2	$K_{om,1}$ (m^3 µg^{-1})	$K_{om,2}$ (m^3 µg^{-1})
Ozone				
Δ^3-Carene	0.128	0.068	0.337	0.0036
α-Pinene	0.125	0.102	0.088	0.0788
β-Pinene	0.026	0.485	0.195	0.0030
Sabinene	0.037	0.239	0.819	0.0001
Nitrate Radical				
Δ^3-Carene	0.743	0.257	0.0088	0 0091
β-Pinene	1.000	-	0.0163	-
Sabinene	1.000	-	0.0115	-

Figure 8. Secondary organic aerosol yields (data and fitted curves) for the bicyclic olefins tested as a function of organic mass concentration in NO_3 experiments. The α_1, α_2, $K_{om,1}$, and $K_{om,2}$ values used to generate the two-product model lines are given in Table 4.
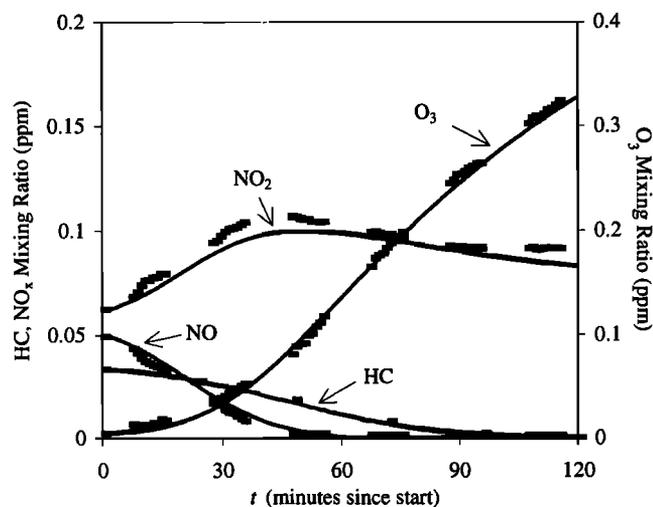
Figure 9. Example output (solid curves) from the SAPRC90b [*Carter*, 1990] gas-phase chemical mechanism. Data (dashes) are shown for the β-pinene experiment performed on July 15, 1997.

sabinene, and Δ^3-carene. By using initial concentrations of hydrocarbon, NO_x, and propene and varying model parameters such as sunlight intensity and temperature, it was possible to simulate experimental concentration profiles of hydrocarbon, NO_x, and O_3, from which it was also possible to infer the amount of hydrocarbon consumed by each oxidant. A sample

output is shown in Figure 9, and the results for the four hydrocarbons tested are summarized in Table 5. As shown in Table 5, the fraction of the parent hydrocarbon consumed by each oxidant varies among compounds and within a set of experiments for a single compound depending on initial concentrations of hydrocarbon and NO_x, sunlight intensity,

Table 5. Simulation of gas-phase chemistry

Date	Parent	ΔHC, ppb	f_{OH},%	f_{O_3},%	f_{NO_3},%	ΔHC$_{OH}$, ppb	ΔHC$_{O_3}$, ppb	ΔHC$_{NO_3}$, ppb
07/01/97a	Δ^3-Carene	28.8	66.4	13 0	19 3	19 1	3.7	5.6
07/01/97b	Δ^3-Carene	66.8	68.1	14.6	13.7	45.5	9.8	9.2
08/21/97b	Δ^3-Carene	72.5	66.0	14.2	18.0	47.8	10.3	13.1
08/15/97b	Δ^3-Carene	73.6	65.9	15 3	15 9	48.5	11.3	11.7
08/19/97b	Δ^3-Carene	104.6	63.4	15.3	19.0	66.3	16 0	19.8
08/17/95a	α-Pinene	73 1	38.3	35 1	24.5	28 0	25.6	17.9
09/22/95b	α-Pinene	90 8	46.0	31 5	21 2	41.7	28.6	19 2
09/22/95a	α-Pinene	94 6	47.4	30.9	20 1	44.8	29.3	19.0
09/25/95b	α-Pinene	94.7	47.8	32 7	18 1	45 3	31.0	17.1
09/25/95a	α-Pinene	96.7	53.0	31 3	14.0	51 3	30.3	13.6
08/15/97a	β-Pinene	32.3	79.6	8 0	9.8	25 7	2.6	3.2
07/15/97a	β-Pinene	33.7	69.0	9.4	19.9	23.2	3.2	6 7
07/17/97a	β-Pinene	42.0	56.6	11.2	31.6	23.8	4.7	13 3
07/27/97a	β-Pinene	45 0	71.4	9 3	17 5	32 1	4.2	7.9
07/15/97b	β-Pinene	62.2	68 6	10 0	18 4	42 7	6.2	11.4
08/19/97a	β-Pinene	79.0	72.0	9 5	15 7	56 9	7 5	12.4
07/21/97a	β-Pinene	85.5	64.3	9 9	23.6	54 9	8.5	20.2
07/21/97b	β-Pinene	96.5	62 9	10.2	24.7	60 7	9 8	23.9
07/09/97a	Sabinene	13 9	69.4	13.5	16.5	9.6	1.9	2.3
07/07/97a	Sabinene	34.9	78 1	14 1	6.5	27.3	4.9	2.3
07/05/97a	Sabinene	53 3	72 4	14 8	10 9	38 6	7.9	5.8
08/24/97b	Sabinene	74.0	73.6	14.7	8.4	54.5	10.9	6.2
07/05/97b	Sabinene	75 3	71.0	14.7	12.7	53.5	11.1	9.6
07/07/97b	Sabinene	77.7	74.5	16.9	5.3	57.9	13.1	4.1
07/09/97b	Sabinene	83.3	71.1	15.0	11 3	59.3	12.5	9.4

and temperature. In addition, it is confirmed that OH is the primary oxidant for all compounds studied under full photooxidation conditions in the chamber.

The fraction of parent hydrocarbon consumed by each oxidant in each photooxidation experiment has been determined for α-pinene, β-pinene, Δ^3-carene, and sabinene. Using experimental data from photooxidation experiments (total amount of organic mass formed and total amount of parent hydrocarbon reacted), yield parameters from ozonolysis experiments, and yield parameters from nitrate radical experiments in conjunction with these data, the contribution of each oxidant to aerosol formation in biogenic photooxidation experiments can be estimated.

By adding the contribution of OH, O_3, and NO_3 to organic aerosol formation in equation (1),

$$Y = \frac{\Delta M_{o,\mathrm{OH}+}}{\Delta HC} + \frac{\Delta M_{o,O_3}}{\Delta HC} + \frac{\Delta M_{o,NO_3}}{\Delta HC} \qquad (5)$$

where OH+ represents OH reaction in addition to any cross reactions (e.g., the reaction of OH with products of initial O_3 reaction). By recognizing that

$$Y_i = \frac{\Delta M_{o,i}}{\Delta HC_i} \qquad (6)$$

with i representing each oxidant, it can be shown that the overall yield is

$$Y = \frac{\Delta M_{o,\mathrm{OH}+}}{\Delta HC} + \sum_i f_i Y_i \qquad (7)$$

where f_i represents the fraction of the parent consumed by oxidant i ($\Delta HC_i / \Delta HC$) for O_3 and NO_3, which has been determined from the gas-phase modeling. By applying (4) to each oxidant, it can be shown that

$$Y_i = \Delta M_o \sum_j \left(\frac{\alpha_{i,j} K_{om,i,j}}{1 + K_{om,i,j} \Delta M_o} \right) \qquad (8)$$

where j now represents each product in the two-product model. Therefore, the overall yield is

$$Y = \frac{\Delta M_{o,\mathrm{OH}+}}{\Delta HC} + \Delta M_o \sum_i f_i \sum_j \left(\frac{\alpha_{i,j} K_{om,i,j}}{1 + K_{om,i,j} \Delta M_o} \right) \qquad (9)$$

with the only unknown being the amount of aerosol organic mass formed from OH reactions and cross reactions, which can be determined for each experiment. The fraction of aerosol derived from the reaction of the parent with each oxidant in photooxidation experiments can then be determined from (6), (8), and (9). The results for each experiment are given in Table 6. It can be seen that the contribution of each oxidant varies among compounds and within a set of compounds for each oxidant. This variation can be explained mechanistically by differences in temperature (affecting kinetics and gas-particle partitioning of secondary products), incident sunlight

Table 6. Individual Contributions to Aerosol Formation

Date	Parent	ΔM_o (μg m^{-3})	Percent Contribution		
			OH	O_3	NO_3
07/01/97a	Δ^3-Carene	2.5	24.14	49.92	25 93
07/01/98b	Δ^3-Carene	11.6	12 48	48 02	39 50
08/21/97b	Δ^3-Carene	54.6	45 23	13.24	41 53
08/15/97b	Δ^3-Carene	63.7	51 52	12 82	35.65
08/19/97b	Δ^3-Carene	99.7	38.25	12.04	49 71
08/17/95a	α-Pinene	22.7	11.75	88 25	0 00
09/22/95a	α-Pinene	33 0	21.04	78 96	0 00
09/25/95b	α-Pinene	34.2	18.70	81.30	0.00
09/22/95b	α-Pinene	38.2	33.48	66.52	0 00
09/25/95a	α-Pinene	39 3	29 34	70.66	0 00
08/15/97a	β-Pinene	7.2	0.00	7.94	92.06
07/15/97a	β-Pinene	14 6	47.66	4 62	47 72
07/17/97a	β-Pinene	20.4	75 86	3 34	20.79
07/27/97a	β-Pinene	34 2	51.97	4.40	43 63
07/15/97b	β-Pinene	51 4	39 62	5.76	54 62
08/19/97a	β-Pinene	100.0	27.78	6.13	66 09
07/21/97a	β-Pinene	109.4	55.97	5.28	38.76
07/21/97b	β-Pinene	141.6	30.30	6.34	63.36
07/09/97a	Sabinene	1.9	74.08	12 01	13 91
07/07/97a	Sabinene	14 3	81.75	6.35	11.90
07/05/97a	Sabinene	23 9	65 98	6 25	27 77
08/24/97b	Sabinene	48.7	71 35	4 41	24.24
07/05/97b	Sabinene	51 4	58.94	4 28	36.78
07/07/97b	Sabinene	53.4	79 33	4 91	15.76
07/09/97b	Sabinene	65.2	62 67	3 92	33.40

intensity (affecting photolysis of NO_3), and initial concentrations (affecting the rate of O_3 and NO_3 formation).

9. Conclusions

The atmospheric aerosol forming potential of 14 of the most prevalent terpenoid biogenic hydrocarbons has been elucidated. Yield parameters for each compound tested show that these compounds have a greater potential to form secondary organic aerosol than typical aromatic constituents of gasoline. Although some degree of grouping of the biogenic hydrocarbons based on structural characteristics in terms of their aerosol forming potentials is possible, this is not uniformly the case at this time. As a result, it will be necessary to account individually for most biogenic hydrocarbons when modeling secondary organic aerosol formation in the ambient atmosphere.

Separate ozonolysis and nitrate radical experiments were performed for bicyclic olefins to investigate aerosol formation from reaction with individual oxidants. Yields in ozonolysis experiments are less dependent on organic mass concentration when compared to those in full sunlight-irradiated photooxidation. Sabinene and β-pinene have significantly lower yields from O_3 reaction alone than the corresponding sunlight-driven photooxidation experiments. However, the opposite behavior is seen for α-pinene and Δ^3-carene. Reaction between NO_3 and β-pinene, Δ^3-carene, or sabinene leads to high conversion to aerosol, indicating probable ambient aerosol formation at night when monoterpenes continue to be emitted and NO_3 accumulates.

It has been confirmed that OH, O_3, and NO_3 each contribute to parent hydrocarbon consumption and aerosol formation in chamber photooxidation. Gas-phase chemistry modeling, combined with yield parameters from individual oxidant experiments, allows for the determination of the contribution of each oxidant to aerosol formation.

References

Alvarado, A., E C Tuazon, S. M Aschmann, R Atkinson, and J Arey, Products of the gas-phase reactions of O(^3P) atoms and O_3 with α-pinene and 1,2-dimethyl-1-cyclohexene, *J Geophys Res, 103*, 25,541-25,552, 1998

Arey, J., A M Winer, R. Atkinson, S M Aschmann, W D Long, and C L Morrison, The emission of (Z)-3-hexen-1-ol, (Z)-3-hexenylacetete, and other oxygenated hydrocarbons from agricultural plant species, *Atmos Environ, 25,* 1063-1075, 1991a

Arey, J., A M Winer, R Atkinson, S M Aschmann, W D. Long, C. L Morrison, and D M. Olszyk, Terpenes emitted from agricultural species found in California's Central Valley, *J Geophys. Res, 96,* 9329-9336, 1991b.

Arey, J., D E Crowley, M. Resketo, and J Lester, Hydrocarbon emissions from natural vegetation in California's South Coast Air Basin, *Atmos Environ, 29,* 2977-2988, 1995

Aschmann, S. M., A Reissell, R Atkinson, and J Arey, Products of the gas-phase reactions of the OH radical with α- and β-pinene in the presence of NO, *J. Geophys. Res, 103,* 25,553-25,561, 1998

Atkinson, R., Gas-phase tropospheric chemistry of volatile organic compounds, 1, Alkanes and alkenes, *J Phys Chem. Ref. Data, 26,* 215-290, 1997

Atkinson, R., J Arey, S. M Aschmann, S. B Corchnoy, and Y. Shu, Rate constants for the gas-phase reactions of *cis*-3-hexen-1-ol, *cis*-3-hexenylacetate, *trans*-2-hexenal, and linalool with OH and NO_3 radicals and O_3 at 296 +/- 2K and OH radical formation yields from the O_3 reactions, *Int. J Chem Kinet, 27,* 941-955, 1995.

Berndt, T., O. Böge, 1 Kind, and W Rolle, Reaction of NO_3 radicals with 1,3-cyclohexadiene, α-terpinene, and α-phellandrene Kinetics and products, *Ber. Bunsen-Ges Phys Chem, 100,* 462-469, 1996.

Calogirou, A., D. Kotzias, and A Kettrup, Atmospheric oxidation of linalool, *Naturwissenschaften, 82,* 288-289, 1995.

Calogirou, A., D Kotzias, and A. Kettrup, Product analysis of the gas-phase reaction of β-caryophyllene with ozone, *Atmos Environ, 31,* 283-285, 1997

Carter, W. P L A detailed mechanism for the gas-phase atmospheric reactions of organic compounds, *Atmos. Environ, 24,* 481-518, 1990.

Chameides, W L, R. W. Lindsay, J Richardson, and C S. Kiang, The role of biogenic hydrocarbons in urban photochemical smog: Atlanta as a case study, *Science, 241,* 1473-1475, 1988.

Chew, A. A, and R. Atkinson, OH radical formation yields from the gas-phase reactions of O_3 with alkenes and monoterpenes, *J. Geophys Res, 101,* 28,649-28,653, 1996

Fehsenfeld, F, et al, Emissions of volatile organic compounds from vegetation and the implications for atmospheric chemistry, *Glob Biogeochem Cycles, 6,* 389-430, 1992

Griesbaum, K, V Miclaus, and I. C. Jung, Isolation of ozonides from gas-phase ozonolyses of terpenes, *Environ Sci Technol., 32,* 647-649, 1998

Grosjean, E, and D Grosjean, The gas phase reaction of unsaturated oxygenates with ozone Carbonyl products and comparison with the alkene-ozone reaction, *J Atmos Chem, 27,* 271-289, 1997.

Guenther, A, et al, A global model of natural volatile organic compound emissions, *J. Geophys. Res., 100,* 8873-8892, 1995.

Hakola, H, J. Arey, S M Aschmann, and R. Atkinson, Product formation from the gas-phase reactions of OH radicals and O_3 with a series of monoterpenes, *J Atmos. Chem., 18,* 75-102, 1994.

Hallquist, M, I. Wängberg, and E. Ljungström, Atmospheric fate of carbonyl oxidation products originating from α-pinene and Δ^3-carene Determination of rate of reaction with OH and NO_3 radicals, UV absorption cross sections, and vapor pressures, *Environ Sci Technol, 31,* 3166-3172, 1997.

Hoffmann, T, J R Odum, F Bowman, D. Collins, D Klockow, R C. Flagan, and J H Seinfeld, Formation of organic aerosols from the oxidation of biogenic hydrocarbons, *J. Atmos. Chem., 26,* 189-222, 1997.

Isidorov, V. A, I G. Zenkevich, and B V. Ioffe, Volatile organic compounds in the atmosphere of forests, *Atmos Environ., 19,* 1-8, 1985

Kaplan, I. R., and R. J. Gordon, Non-fossil-fuel fine-particle organic carbon aerosols in southern California determined during the Los Angeles aerosol characterization and source apportionment study, *Aerosol Sci Technol., 21.* 343-359, 1994

König, G, M Brunda, H Puxbaum, C N Hewitt, S. C. Duckham, and J Rudolph, Relative contribution of oxygenated hydrocarbons to the total biogenic VOC emissions of selected mid-European agricultural and natural plant species, *Atmos Environ., 29,* 861-874, 1995

Lamb, B., D. Gay, H Westberg, and T. Pierce, A biogenic hydrocarbon emission inventory for the U S A. using a simple forest canopy model, *Atmos Environ., 27,* 1673-1690, 1993

Leaitch, W R, J W Bottenheim, T A Biesenthal, S. M Li, P. S K Liu, K Asalien, H. Dryfhout-Clark, F Hopper, and F. Brechtel, A case study of gas-to-particle conversion in an eastern Canadian forest, *J Geophys Res,* in press, 1998

McKeen, S A, E Y Hsie, and S C Liu, A study of the dependence of rural ozone on ozone precursors in the eastern United States, *J. Geophys Res, 96,* 15,377-15,394, 1991

Muller, J F, Geographical distribution and seasonal variation of surface emissions and deposition velocities of atmospheric trace gases, *J Geophys Res, 97.* 3787-3804, 1992.

Odum, J. R, T Hoffmann, F. Bowman, D Collins, R C. Flagan, and J. H Seinfeld, Gas/particle partitioning and secondary organic aerosol yields, *Environ Sci Technol, 30,* 2580-2585, 1996.

Odum, J R, T. P. W Jungkamp, R J. Griffin, R C. Flagan, and J H. Seinfeld, The atmospheric aerosol-forming potential of whole gasoline vapor, *Science, 276,* 96-99, 1997a.

Odum, J R, T. P. W Jungkamp, R J. Griffin, H J. L Forstner, R C Flagan, and J H. Seinfeld, Aromatics, reformulated gasoline, and

atmospheric organic aerosol formation, *Environ Sci Technol, 31,* 1890-1897, 1997b

Pandis, S N , S E Paulson, J. H Seinfeld, and R C Flagan, Aerosol formation in the photooxidation of isoprene and β-pinene, *Atmos Environ., 25,* 997-1008, 1991

Pandis, S N., R. A Harley, G R Cass, and J H Seinfeld, Secondary organic aerosol formation and transport, *Atmos. Environ , Part A, 26,* 2269-2282, 1992

Pankow, J. F An absorption model of the gas/aerosol partitioning of organic compounds in the atmosphere, *Atmos. Environ., 28,* 185-188, 1994a

Pankow, J. F. An absorption model of the gas/aerosol partitioning involved in the formation of secondary organic aerosol, *Atmos. Environ, 28,* 189-193, 1994b.

Puxbaum, H , and G Konig, Observation of dipropenyldisulfide and other organic sulfur compounds in the atmosphere of a beech forest with *allium ursinum* ground cover, *Atmos Environ , 31,* 291-294, 1997.

Roselle, S. J , T E. Pierce, and K L Schere, The sensitivity of regional ozone modeling to biogenic hydrocarbons, *J Geophys Res , 96,* 7371-7394, 1991.

Schauer, J J , W. F Rogge, L. M Hildemann, M A Mazurek, G R Cass, and B R T. Simoneit, Source apportionment of airborne particulate matter using organic compounds as tracers, *Atmos. Environ , 30,* 3837-3855, 1996

Seinfeld, J H , and S N Pandis, *Atmospheric Chemistry and Physics,* Wiley-Interscience, New York, 1998.

Shu, Y , and R Atkinson, Atmospheric lifetimes and fates of a series of sesquiterpenes, *J Geophys. Res , 100,* 7275-7281, 1995.

Shu, Y , E. S C. Kwok, E C Tuazon, R Atkinson, and J Arey, Products of the gas-phase reactions of linalool with OH radicals, NO3 radicals, and O3, *Environ Sci Technol., 31,* 896-904, 1997

Stephanou, E G , and N. Stratigakis, Oxocarboxylic and α, ω-dicarboxylic acids Photooxidation products of biogenic unsaturated fatty acids present in urban aerosols, *Environ. Sci. Technol , 27,* 1403-1407, 1993.

Turpin, B. J., and J. J Huntzicker, Identification of secondary organic aerosol episodes and quantitation of primary and secondary organic

aerosol concentrations during SCAQS, *Atmos Environ , 29,* 3527-3544, 1995.

Vinckier, C , F. Compernolle, and A M. Saleh, Qualitative determination of the non-volatile reaction products of the α-pinene reaction with hydroxyl radicals, *Bull Soc. Chim Belg , 106,* 501-513, 1997

Wängberg, I., I. Barnes, and K H Becker, Product and mechanistic study of the reaction of NO3 radicals with α-pinene, *Environ Sci Technol , 31,* 2130-2135, 1997

Wang, S C , and R C Flagan, Scanning electrical mobility spectrometer, *Aerosol Sci Technol , 13,* 230-240, 1990.

Went, F W Blue hazes in the atmosphere, *Nature, 187,* 641-643, 1960.

Winer, A. M., J Arey, R. Atkinson, S M. Aschmann, W D Long, C L Morrison, and D. M Olszyk, Emission rates of organics from vegetation in California's Central Valley, *Atmos. Environ , 26,* 2647-2659, 1992.

Yu, J., R C. Flagan, and J. H. Seinfeld, Identification of products containing -COOH, -OH, and -C=O in atmospheric oxidation of hydrocarbons, *Environ Sci Technol , 32,* 2357-2370, 1998

Zhang, S H , M Shaw, J H. Seinfeld, and R C Flagan, Photochemical aerosol formation from α-pinene and β-pinene, *J Geophys Res , 97,* 20,717-20,729, 1992

D.R. Cocker III, Department of Environmental Engineering Science, California Institute of Technology, 1200 E. California Blvd., Mail Code 138-78, Pasadena, CA 91125. (e-mail: cocker@cco.caltech.edu)

R.C. Flagan and R.J. Griffin, Department of Chemical Engineering, California Institute of Technology, 1200 E. California Blvd., Mail Code 210-41, Pasadena, CA 91125. (e-mail: flagan@cheme.caltech.edu; robert@cco.caltech.edu)

J.H. Seinfeld, Division of Engineering and Applied Science, California Institute of Technology, 1200 E. California Boulevard, Mail Code 104-44, Pasadena, CA 91125. (e-mail: seinfeld@cco.caltech.edu)